



BNL-221280-2021-TECH

NSRL-TN-05-002

Time of Flight of NSRL Beams

I. Chiang, A. Rusek

October 2005

Collider Accelerator Department
Brookhaven National Laboratory

U.S. Department of Energy

USDOE Office of Science (SC), Nuclear Physics (NP) (SC-26)

Notice: This technical note has been authored by employees of Brookhaven Science Associates, LLC under Contract No. DE-AC02-98CH10886 with the U.S. Department of Energy. The publisher by accepting the technical note for publication acknowledges that the United States Government retains a non-exclusive, paid-up, irrevocable, world-wide license to publish or reproduce the published form of this technical note, or allow others to do so, for United States Government purposes.

DISCLAIMER

This report was prepared as an account of work sponsored by an agency of the United States Government. Neither the United States Government nor any agency thereof, nor any of their employees, nor any of their contractors, subcontractors, or their employees, makes any warranty, express or implied, or assumes any legal liability or responsibility for the accuracy, completeness, or any third party's use or the results of such use of any information, apparatus, product, or process disclosed, or represents that its use would not infringe privately owned rights. Reference herein to any specific commercial product, process, or service by trade name, trademark, manufacturer, or otherwise, does not necessarily constitute or imply its endorsement, recommendation, or favoring by the United States Government or any agency thereof or its contractors or subcontractors. The views and opinions of authors expressed herein do not necessarily state or reflect those of the United States Government or any agency thereof.

Time of Flight Measurement of NSRL beams

I-Hung Chiang, Adam Rusek, M. Sivertz

Motivation

For most applications, NSRL Users are interested in only the nominal kinetic energy of the beam particles, and precision given by Bragg curve measurements or RF system measurements are unnecessary. There are some applications for which it may be necessary to measure the beam energy via time-of-flight (ToF) techniques such as proton beams that cannot be measured at NSRL with a Bragg curve.

The study of fragmentation products may also benefit from a good measurement of the kinetic energy of the fragments.

Apparatus

The ToF detector is very simple. It consists of two small scintillator paddles, S1 and S2 (3.175 cm x 3.175 cm x 0.2 cm thick) connected by a Lucite light guide to a photomultiplier tube (PMT). The PMTs are mounted on frames that sit on the rails in the target room. The signals from both PMTs are brought to the NSRL control room where they are passively split. Half the signal goes to a pulse height compensated discriminator with a 4ns long trim cable, the output of which enters a TDC. The other half is delayed in ~100ns cable before it enters a QDC. The trigger for the data acquisition is provided by the discriminated S1 signals. The trigger provides both the TDC-Start and the QDC-Gate, as well as begins the readout of the VME system.

The detectors are set up on the rails close to each other, ~10 cm from each other, and a careful measurement is made of the location of the S2 scintillator frame. Data are collected in this configuration. Then S2 is moved to a new location a well measured distance away, typically several meters, and more data are collected. The change in the time response of S2 gives the time of flight between the two locations. Additional corrections may be required (see below).

Pulser calibration of TDC

The CAEN V775N TDC has a nominal calibration of 35 ps/bin when operating in its most sensitive setting, when the Full Scale Range Register (FSRR) is set to 255. Most of our data were collected at this setting. This calibration was checked by using a Stanford Research Systems DG535 Delay/Pulse Generator, by varying the time delay between the Start and Stop pulses. A linear fit (Figure 1) gives a calibration of 35.8 ps/bin, close to the nominal value. Typical delay accuracy for the DG535 is 500ps for the delay range used in this test, although the resolution is listed as 5ps. Figure 1b shows the residuals after the linear fit. The structure is not statistical, but shows a reproducible shape.

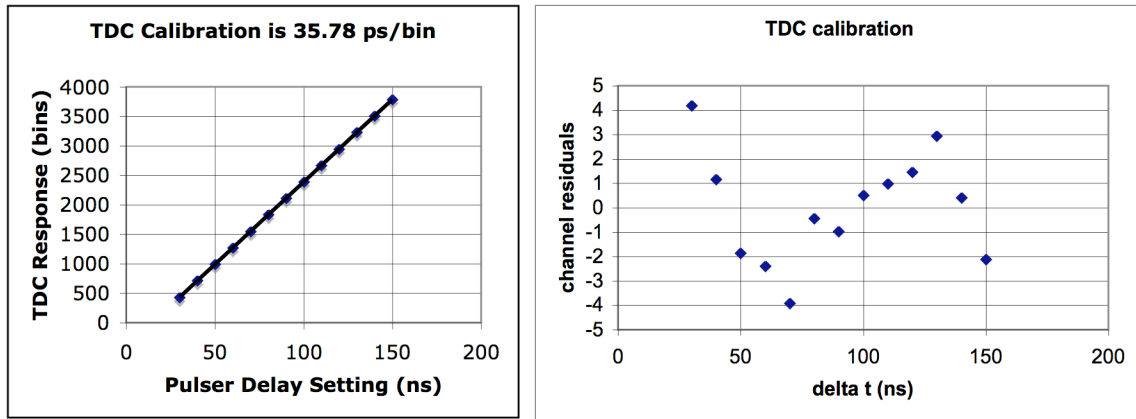


Figure 1: Calibration of TDC with a precision pulser showing (a) the linear relationship, a conversion factor of 35.78 ps/bin, and (b) the non-statistical structure of the residual distribution.

RF calibration of TDC

We attempted to make an independent measurement of the TDC calibration based on the RF time structure of the beam. On 7 October 2005, while running 1000 MeV protons, we misaligned the two scintillators so a single beam particle would not pass through both. Then we adjusted the beam intensity until we were triggering on a beam particle for about half of every booster cycle, 385.245 ns (2.59575 MHz) and recorded the TDC spectrum. This spectrum (Figure 2) shows two peaks, one where S2 saw a proton in the same booster bunch as the trigger proton, and a second peak when the proton in S2 was from the following booster bunch, 385 ns later. Unfortunately because the two peaks are separated by such a large time interval, the TDC had to operate in a non-standard configuration with a FSRR setting of 60 instead of the standard 255. The TDC manual specifies that the calibration should scale like $1/\text{FSRR}$, for a calibration of $255/60 \times 35\text{ps} = 148.75\text{ps/bin}$.

The two peak locations (bins 401 and 3005) and the time difference between booster bunches determines the TDC calibration for a FSRR setting of 60: 147.85 ps/bin, in reasonable agreement with the result obtained by scaling. The effect of running the PMTs at a low voltage (-900 volts) and a high rate (2 MHz) may also have affected the results. The peak shapes reflect the time of arrival of the first proton from a booster bunch at a scintillator, and these shapes are not Gaussian at all.

When this calibration was used to measure 1000 MeV proton ToF on 9 October 2005, it gave a result of 942 MeV whereas the 35.8ps/bin calibration gave 957 MeV. This effort needs to be revisited.

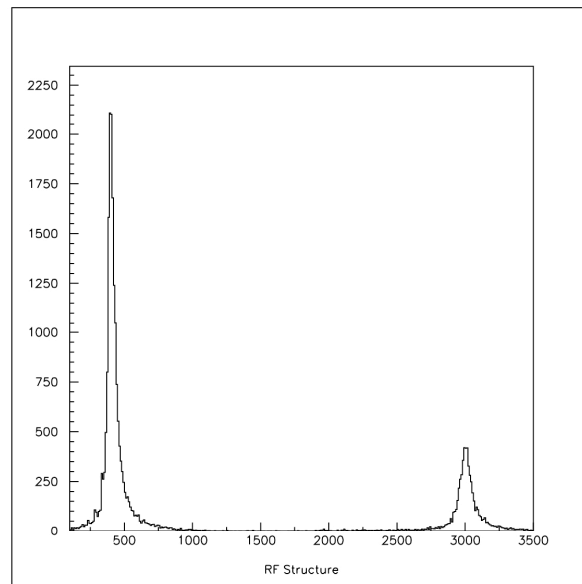


Figure 2: Double pulse structure due to Booster RF.

ToF Measurement Summary

Table 1 shows a summary of the ToF results obtained for three different species of ion. The most accurate energy measurement comes from the Booster RF. The Bragg peak is also probably accurate to 0.5 MeV per nucleon where it can be used.

Before comparing the RF energy to the ToF energy, a correction needs to be applied for the energy loss between the booster and the scintillator. This includes (for the Fe and Ti) a Cu foil 0.05cm thick, and Al vacuum window, 0.05cm thick, up to 10m of air, and for some of the data taking (red) beam particles traveled through the camera flag and mirror (treated as 0.71cm Si). The mirror correction should not be applied when comparing the RF result to the Bragg peak result, since this is upstream of the camera. Energy loss corrections are small for protons, but can be substantial for Fe and Ti, as shown in Table 2.

Date	Ion	KE(RF) MeV/N	dE/dx corrected	KE (Bragg)	KE (ToF)
13-Oct-05	Ti	1007.6	992.7	979.9	965.9
12-Oct-05	Ti	1007.6	971.8	979.9	966.7
9-Oct-05	Ti	1007.6	971.8	979.9	955.6
18-Oct-05	Fe	611.66	591.0	585.1	595.3
4-Oct-05	H	991.7	988.5	---	979.1
	H	989.6	986.4	---	979.5
	H	988.5	985.3	---	948.4

Table 1: Comparison of Time-of-Flight measurement of beam kinetic energy versus the KE derived from Booster RF and the Bragg peak. (See Appendix X for complete data.)

In general the Bragg peak measurements and the RF results are in agreement at the 1% level. The resolution of the RF energy measurement is limited by the knowledge of the orbits in the Booster. Typical RF energies are quoted with an accuracy of 0.1 MeV. The Bragg peak measurements have proven to be very reproducible, with peaks observed at the same location over many days of running. The finest granularity of the Bragg peak measurement is the 0.025 cm sheet of polyethylene, which corresponds to a step in KE of ~0.25 MeV, depending on the ion species and the beam energy. ToF results are not in as good agreement with either the RF or the Bragg peak, and appear to fluctuate on the 1-2% level. More systematic studies need to be conducted to understand the limitations of this method. Complete data are presented in Appendix A.

Ion	Energy (MeV/N)	dE/N (Total)	LET (Air)	dE/N (Air)	LET (Cu)	dE/N (Cu)	LET (Al)	dE/N (Al)	LET (Camera)	dE/N (Camera)
Ti	1000	14.9	945	5.5	751	7.0	857	2.4	913	29.4
Ti	1000	35.8	945	11.7	751	7.0	857	2.4	913	29.4
Ti	1000	35.8	945	11.7	751	7.0	857	2.4	913	29.4
Fe	600	20.6	1521	7.8	1198	9.5	1374	3.3	1467	40.5
H	1000	3.2	1.956	1.5	1.554	0.7	1.77	0.2	1.886	2.9

Table 2: Energy loss (per nucleon) for Ti, Fe and H ions when passing through air, Cu, Al, and Si barriers as well as the total dE/dx per nucleon prior to a ToF measurement. Also shown are the LET values for those ions.

Subtracting (or not) the T0 pulse?

What is the best way to measure the ToF? Using S1 as a TDC Start, and S2 as the TDC Stop for TDC Channel 0 (TDC-0) seems like the most straightforward approach. The TDC-0 may have systematic shifts, so a copy of S1 was put into TDC-1. TDC-1 should be constant since the same signal provides both the Start and Stop. Although the TDC-1 distribution is quite narrow (35ps RMS) there is a clear correlation between the TDC-0 time and the TDC-1 time, as is shown in Figure X. This indicates that the TDC itself has a behavior that systematically shifts the calibration of the TDC as a whole. This could be related to temperature fluctuations, power supply levels or a number of other causes.

As a result of this observation, we tried obtaining the time of flight by subtracting fluctuations in the TDC-1 Start time from the TDC-0 Stop time, correcting for the TDC shifts in calibration. This had the expected result of making the TDC-0 Stop distribution narrower, from 45ps to 40ps. But there was an additional oddity observed. There seemed to be a systematic shift in the TDC-1 value depending on the TDC-0 value, as if there were a kind of cross-talk between channels of the TDC. We attempted to understand the source of this discrepancy by observing the TDC response to a pulser with a variable delay between 0 and 20 ns on the input to TDC-0, keeping the input to TDC-1 fixed, mimicking the ToF data. In the initial study there appeared to be systematic shifts on the order of 2 to 3 bins (70-100ps). Since we could not rule out cross-talk in the pulser providing the TDC Start and Stop, we repeated the study using cable delays instead of pulser delays. When using cable delays, we could not reproduce the shifts seen with the pulser.

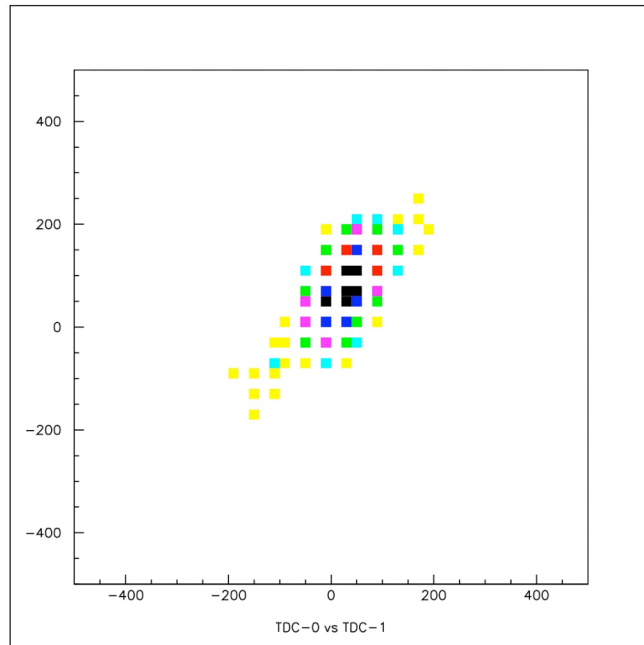


Figure 3: Correlation between TDC-0 and TDC-1. Axes are in picoseconds.

Errors and Uncertainties

Since the measurement is such a simple one, the only source for uncertainties is from the distance between scintillator measurements, L , and the time it takes to make the trip, $t = L/\beta c$. The error in t comes from measurement error of the peak TDC bin, B , which can be reduced to an arbitrarily small amount by taking many events making the statistical uncertainty negligible. But there is a contribution to the time error that comes from the calibration constant of the TDC, C , $t = BC$. This is systematic. Presumably we could use the beam to calibrate; i.e. take a measurement of the kinetic energy using the RF or the Bragg peak, and use that value to define the TDC calibration. Then we would need to be concerned only about the reproducibility and stability of that calibration.

In general, the fractional error on the beam energy depends on the fractional error in time and distance in the following manner:

$$\sigma(E)/E = \gamma^2 \beta^2 \sqrt{(\sigma(B)^2/B^2 + \sigma(C)^2/C^2 + \chi(L)^2/L^2)} \quad \text{Eq 1}$$

where E is the total energy of the beam particle, $\sigma(E)$ is the error in E , and B , C , and L refer to the error in the TDC peak, TDC calibration, and Distance measurement respectively. In a typical measurement of a proton beam of 1 GeV kinetic energy, γ has a value of ~ 2 , while β is near 1 amplifying the fractional error by a factor of ~ 4 . Converting to an error on the kinetic energy only makes the amplification greater. An error of 1% in each of B , C , and L makes for an error of over 6% in the KE. Fractional errors in B for this data set were on the order of 10^{-4} and in principle can be reduced by taking more events. Similarly, fractional errors in L were 5×10^{-4} and could be reduced by using longer flight distances. But the error in C is probably on the order of 1%, and it is not clear how to reduce it. The best hope lies in making use of a known beam energy to calibrate the TDC, and testing to ensure the calibration stays constant.

In a test of this technique, a series of ToF measurements was made on an Fe beam at 600 MeV nominal KE. Six independent results gave a mean of 595.3 MeV to compare with 591.0 MeV from the RF (corrected for losses). The RMS of the 6 results was 0.6 MeV, indicating that a good calibration obtained from beam could give a stable reproducible ToF energy mechanism.

Action Items

- 1) Reproduce the TDC calibration using a different delay pulse generator.
- 2) Reproduce the TDC calibration using booster bunch separation.
- 3) Calibrate the TDC using beam, and verify reproducibility and internal consistency of ToF measurements.
- 4) Revisit the cross-talk study with the new high-resolution TDC.

Appendix A: Data used in Time of Flight Calculation

Ion	Z	A	Most abundant isotope (AMU)	Mass(MeV)	(Mass-Z*m _e)/AMU
p	1	1	1	938.27	938.27
H	1	1	1.008	938.95	938.43
Ti	22	48	47.983	44695.88	930.93
Fe	26	56	55.935	52103.12	930.18

Table 3: Masses for ToF calculation: Mass per AMU with electron mass subtracted.

Material	Density (g/cc)	Thickness (cm)
Cu (foil)	8.92	0.05
Al (window)	2.7	0.05
Air	0.0012	233 to 643
Si (Camera)	2.18	0.71*

*Half of the dE/dx in Camera is used since approximately half the flight path is after Camera and half before.

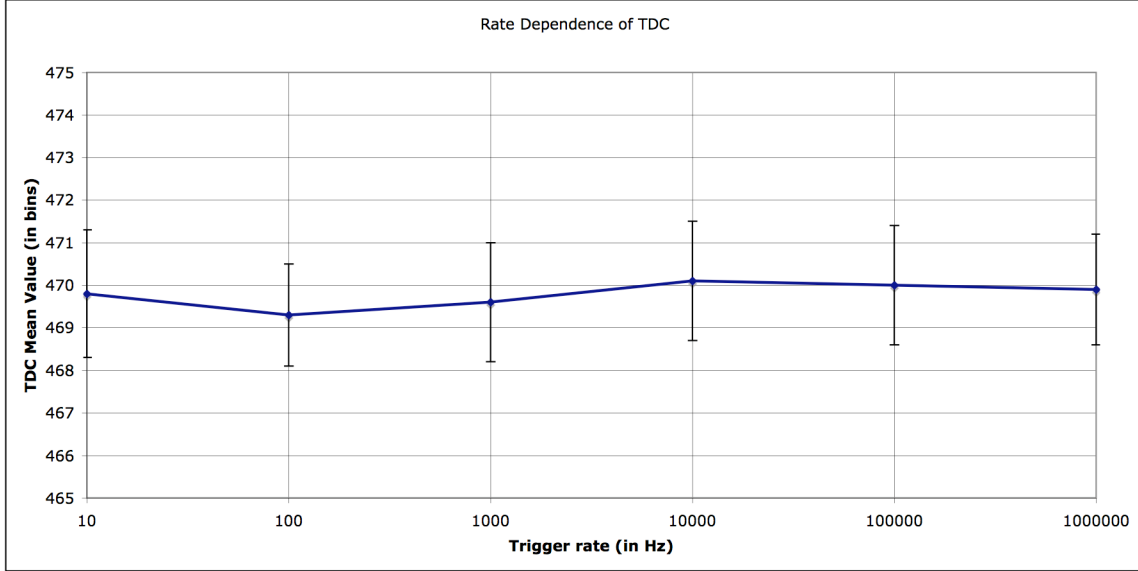
Table 4: Materials taken into consideration in the dE/dX losses, giving the density, and thicknesses.

Date	Ion	Location (inches)	Distance (cm)	<tdc1> peak	ToF (ps)	β	Kinetic Energy
18-Oct-05	Fe	129	177.8	692.32	7485	0.7923	594.5
	Fe	59	177.8	483.24	7490	0.7918	592.7
	Fe	129	177.8	692.46	7477	0.7932	597.3
	Fe	59	177.8	483.61	7474	0.7935	598.3
	Fe	129	177.8	692.38	7487	0.7921	593.7
13-Oct-05	Ti	126	172.72	1225.6	6612	0.8713	965.2
	Ti	58	-----	1040.9	-----	-----	-----
12-Oct-05	Ti	284	449.58	1692.0	17209	0.8714	966.0
	Ti	107	-----	1211.3	-----	-----	-----
9-Oct-05	Ti	284	449.58	449.5	17290	0.8673	938.8
	Ti	107	----	332.6	----	----	----
	Ti	284	----	1674.8	17241	0.8698	954.9
	Ti	107	----	1193.2	----	----	----
4-Oct-05	H	283	152.4	597.15	5859	0.8676	948.4
	H	223	----	433.48	----	----	----

Table 5: Data summary from ToF running. All runs had FSRR=255 (35.8 ps/bin) except the runs in red (FSRR=60, 148 ps/bin).

Appendix B: Rate dependence of TDC

We studied the TDC dependence on input rate by prescaling the trigger/readout rate in decades from 10 Hz to 1 MHz. The readout rate stayed fixed at 10 Hz. No dependence was observed.



Trigger Rate (Hz)	Peak position (in bins)	Width (in bins)
10	469.8	1.5
100	469.3	1.2
1,000	469.6	1.4
10,000	470.1	1.4
100,000	470	1.4
1,000,000	469.9	1.3

Table 6: Rate dependence of TDC performance.